Solution and Film Properties of Sodium Caseinate/Glycerol and Sodium Caseinate/Polyethylene Glycol Edible Coating Systems

Diana C. W. Siew,*,†,‡ Carola Heilmann,† Allan J. Easteal,§ and Ralph P. Cooney§

Industrial Research Limited, P.O. Box 2225, Auckland, New Zealand, and Department of Chemistry, The University of Auckland, Private Bag 92019, Auckland, New Zealand

The aim of this study is to determine the effects of plasticizer hydrogen bonding capability and chain length on the molecular structure of sodium caseinate (NaCAS), in NaCAS/glycerol and NaCAS/polyethylene glycol 400 (PEG) systems. Both solution and film phases were investigated. Glycerol and PEG reduced the viscosity of aqueous NaCAS, with the latter having a greater effect. This was explained in terms of protein/plasticizer aggregate size and changes to the conformation of the caseinate chain. In the film phase, glycerol caused more pronounced changes to the film tensile strength compared with PEG. However, the effect of glycerol on film water vapor permeability was smaller. These observations are attributed to the differences in plasticizer size and hydrogen bonding strength that controls the protein−plasticizer and protein−protein interactions in the films. Glass transition calculations from the tensile strength data indicate that the distribution of bonding interactions is more homogeneous in NaCAS/PEG films than in NaCAS/glycerol films.

Keywords: *Edible coatings; sodium caseinate; films; solution; properties*

INTRODUCTION

There has been a resurgence of interest in recent years in the development of edible coatings for food (Debeaufort et al., 1998; Miller and Krochta, 1997), in particular for prolonging the storage life of fresh fruits and vegetables and retaining freshness in taste and appearance (Krochta et al., 1994; Nisperos and Baldwin, 1996; Nussinovitch and Lurie, 1995). Motivation for this work has come from consumer pressures in relation to health, food quality, convenience, increased purchasing power, and more proactive attitudes toward reducing the environmental impact of packaging wastes.

Several studies have indicated the potential of milk proteins for use with horticulture products (McHugh and Krochta, 1994a,b; Krochta et al., 1990; Gennadios et al., 1994; Avena-Bustillos et al., 1993, 1994). The suitability of milk proteins is based on its nutritional value and several key physical characteristics for effective performance in edible films. As with other protein coatings, milk protein films have good mechanical characteristics, and appropriate O_2 and CO_2 permeabilities, particularly at low humidity levels: the main disadvantage is their poor water barrier properties. Commercial exploitation of milk protein films hinges on reducing the sensitivity of the films to moisture. Approaches that have been reported for achieving reduced water sensitivity are, broadly, as follows. The first emphasizes increasing the cohesion of the protein chains, most commonly achieved through metal ion and enzymic cross-linking (Avena-Bustillos and Krochta, 1993; Motoki et al., 1987) or γ-irradiation-induced cross-linking (Mezgheni et al., 1998). The second approach exploits the amphiphilic nature of milk proteins in emulsion films with other polysaccharide and lipid materials, to form coatings that combine the strength, appearance, good gas permeability characteristics, and adhesion properties of milk protein films with favorable water barrier properties (McHugh and Krochta, 1994a). To date, a water-soluble coating with good water barrier properties has not been developed (Nussinovitch and Lurie, 1995). Progress in this field will occur as protein functional properties and chemical interactions between the protein and other film-forming materials are better understood. An impetus is the introduction of new biopolymer derivatives.

The simplest edible film formulation involves the addition of a plasticizer to the base polymer to alter the mechanical and physical characteristics (in particular, flexibility, toughness, tear resistance, and gas permeability) of the film. This study focuses on two protein/plasticizer systems: sodium caseinate (NaCAS) with (a) glycerol and (b) polyethylene glycol (PEG; molecular weight = 400), as plasticizers. Both materials are U.S. FDA approved additives (U.S. FDA, 1997) commonly used in food coatings.

The aim of this work was to elucidate the molecular interactions between the components of an edible film for tailoring of specific-purpose films. The effects of plasticizer hydrogen bonding properties and chain lengths on the molecular structure of the caseinate chains are compared to determine the relationship between protein structure, film properties (including tensile strength and water vapor permeability), and properties of the caseinate/plasticizer mixtures in solution. The long-term objective is to utilize the results obtained from the present study and related work in progress (Siew et al., 1999) to construct predictive models for specific function films.

* Author to whom correspondence should be addressed (fax 649-307 0618; e-mail d.siew@mpt.co.nz).
† Industrial Research Limited.
‡ Present address: Materials Performance Technologies, P.O. Box 2225, Auckland, New Zealand.
§ The University of Auckland.

10.1021/jf9806311 CCC: $18.00
Published on Web 07/27/1999

Table 1. Statistical Distribution of the Principal Components in Casein and Sodium Caseinate

casein component	% component of skim milk protein, %x[a]	approx MW(x)[a]	av no. of phosphate groups per casein component	no. of Na^+ ions associated with the caseinate form, $N(Na^+)_x$[b]
α-casein	50	23500	11	11
β-casein	35	24000	5	4
κ-casein	15	19000	1	1

[a] x represents the various α-, β-, or κ-casein fractions. [b] The number of Na^+ ions, $N(Na^+)_x$, associated with the caseinate form of each component is calculated as follows: $N(Na^+)_x = 2N(PO_4)_x(\%x)$, where $N(PO_4)$ is the number of phosphate groups associated with each component and %x is the percentage of the α-, β-, or κ-casein component. $N(Na^+)_x$ is then approximated to the nearest whole number.

MATERIALS AND METHODS

Materials. Sodium caseinate (NaCAS) (Alanate 180) was kindly supplied by the New Zealand Dairy Board. Glycerol and polyethylene glycol (PEG; MW = 400) (BDH products) were dried over molecular sieves prior to use. All solutions were made with distilled water.

Solution Preparation Method. The NaCAS/plasticizer systems were made up with constant total mass (50 g). Each solution contained 10 wt % of NaCAS and plasticizer concentrations in the concentration range 0.01−0.26 mol of glycerol/100 g of solution or 0.003−0.059 mol of PEG/100 g of solution. The NaCAS content ranged from 10.0 to 11.8% when expressed as a weight ratio of the protein and water components only.

The aqueous mixture of protein and plasticizer was stirred for ∼1 h to obtain a homogeneous solution. This was used either fresh or after a maximum of 3 days of storage at 5 °C. The viscosity of the protein solutions remained unchanged for up to 3 days at this temperature, indicating that no aging effects occurred during this time.

The glycerol and PEG systems were formulated so that the plasticizer−oxygen concentration was similar to facilitate comparison between the two systems. The units adopted to reflect this are expressed as *moles of plasticizer−oxygen atoms per mole of NaCAS*, where the unit *moles of plasticizer−oxygen atoms* was obtained by multiplying the number of moles of plasticizer with the number of oxygen atoms attached to the plasticizer molecular skeleton. The molecular weight of NaCAS was theoretically estimated from the statistical ratio of the principal components of casein, i.e. α-, β-, and κ-casein, reported in the literature (Kinsella, 1984) and assuming that each phosphate group attached to the various casein components is associated with two Na^+ atoms (Table 1). The average molecular weight of NaCAS was estimated as 23368

$$\mathrm{MW(NaCAS)} = (\%\alpha)[\mathrm{MW}(\alpha)] + (\%\beta)[\mathrm{MW}(\beta)] + (\%\kappa)[\mathrm{MW}(\kappa)] + N(Na^+)_\alpha[\mathrm{MW(Na)}] + N(Na^+)_\beta[\mathrm{MW(Na)}] + N(Na^+)[\mathrm{MW(Na)}] \quad (1)$$

where MW(NaCAS), MW(α), MW(β), MW(κ), and MW(Na), respectively, represent the molecular weights of NaCAS, α-, β-, and κ-casein, and Na; %α, %β, and %κ are the various casein fractions; and $N(Na^+)_\alpha$, $N(Na^+)_\beta$, and $N(Na^+)_\kappa$ are the numbers of Na^+ ions associated with the caseinate form of the various casein components (Table 1).

Film Formation Method. Films were made by pouring the film-forming solution (40 mL) in a flat 17 × 27 cm polycarbonate tray or (4.5 mL) in an 8 cm diameter polycarbonate Petri dish sitting on a level surface. The solution was spread evenly over the whole surface area and allowed to dry in an oven at 35 °C for 24 h. Clear transparent films that could be removed easily and intact from the surface were formed in most cases. All films were used within 5 days of preparation and, prior to conditioning for the various experiments, desiccated under ambient conditions.

Film Thickness Measurements. Film thickness was determined to ±1 μm using a hand-held digital micrometer from 10 readings taken at random over the film surface. The average film thickness was ∼85 μm. Films with similar thicknesses were used within a set of experiments. Film thickness was measured before and after water vapor permeability tests and after equilibration at 50% relative humidity (RH) for tensile property determination.

Solution Viscosity and Density Measurements. The viscosity of the NaCAS solutions was determined at 25 °C with an Ubbelohde-type capillary viscometer with viscometer constant 9.8259×10^{-4} S s^{-1}. Kinematic viscosity, ν, was calculated from the average of three flow time measurements for each solution, and absolute viscosity, η, was evaluated from the relationship $\eta = \nu\rho$ (where ρ = density).

A vibrating tube densimeter (Anton Paar Model DMA 02C) was used to determine the density of the solutions at 25 °C. Two liquids with accurately known densities (water and 20 wt % sucrose in water) were used to calibrate the densimeter.

Tensile Properties. The tensile strength and percentage elongation-at-break of the NaCAS films were determined according to the standard method ASTM D882-91 using an Instron tester, Model 1026. Film samples (10 cm × 2.54 cm strips) were preconditioned at 23 ± 2 °C and 50 ± 5% RH for 48 h prior to tensile measurement. Five samples of each film were tested. The initial grip separation and crosshead speed used were 50 mm and 500 mm min^{-1}, respectively.

Water Vapor Permeability (WVP) Determination. Test cells based on a reported design (Park, J. W., et al., 1994) were used: the method is a variation of the *cups method* described in ASTM E96-80. The cells were cylindrical cups made from poly(methyl methacrylate), with i.d. = 4.6 cm, o.d. = 8.7 cm, and depth = 2.1 cm. The lids were filled with dried silica gel and covered with a film sample. The film was clamped between the cup and a 0.5 cm thick lid, and the lid was attached to the cup with four screws placed symmetrically around the cup perimeter. After the film samples were mounted, the assembly was weighed and placed in a chamber maintained at 45% RH (using saturated K_2CO_3 solution) and 20 °C. The cells were weighed daily until the color of the silica gel changed from blue to pink. This occurred between 1 and 2 weeks, depending on the film formulation. The WVP reported here is an average of at least three samples per formulation.

WVP was calculated using the equation

$$\mathrm{WVP\ (ng\cdot m\cdot m^{-2}\cdot Pa^{-1})} = 10^9\{[(d \times 10^{-3})(w_f - w_s)]/[3600 t a_f[p(\mathrm{RH_o}) - p(\mathrm{RH_i})]]\} \quad (2)$$

where d is the thickness of the film at the end of the experiment (mm), w_s and w_f are the initial and final weights of the cells (g), t is the exposure time (h), a_f is the area of exposed film (m^2), p is the vapor pressure of the saturated solution at 20 °C, and RH_o and RH_i are the respective relative humidity values outside and inside the cell.

FTIR Spectroscopic Analysis. FTIR spectra were recorded using a Digilab FTS-60 FTIR spectrometer equipped with an MCT detector. Spectra of the solution phase were obtained in the transmission mode using thin films between CaF_2 windows at 2 cm^{-1} resolution. A known volume of solution was spread evenly onto the window to create the thin film. A solution cell was not used as there was difficulty in injecting the sample into the cell due to the viscosity of the solutions. Each spectrum is the result of 800 co-added scans.

Spectra were analyzed using the SpectraCalc GRAMS/386 software. All spectra were initially baseline corrected between 2900 and 1200 cm^{-1} and then normalized with respect to the libration mode of water at 2130 cm^{-1}. The contribution from the bending mode of water at 1645 cm^{-1} to the intensity of the amide I [ν(C═O)] band of NaCAS between 1600 and 1700 cm^{-1} was removed by completely suppressing the 2130 cm^{-1} band using the spectrum of water as subtraction reference. Residual water vapor bands were removed by a second subtraction, if required, using the spectrum of water vapor as the reference. The resultant difference spectra were smoothed

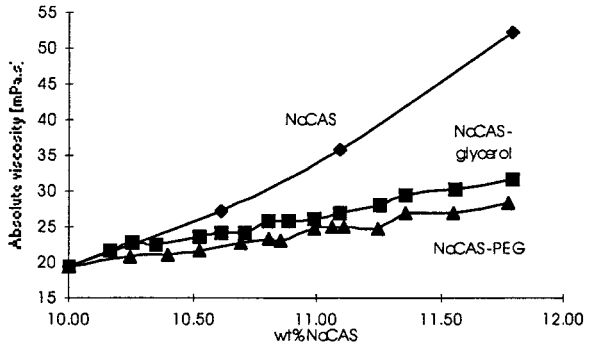

Figure 1. Effect of glycerol and PEG on the viscosity of aqueous NaCAS at 25 °C.

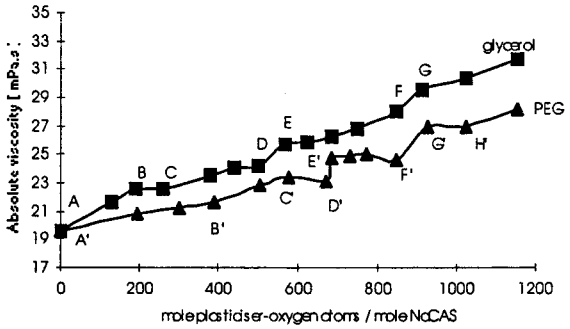

Figure 2. Viscosity trends (25 °C) in NaCAS/plasticizer systems. The standard deviations associated with the data are ±0.058 and ±0.083 mPa•s, respectively, for the glycerol and PEG systems.

with a nine-point Savitsky−Golay function (Savitsky and Golay, 1964; Madden, 1978) and used to generate second-derivative spectra using the Savitsky−Golay derivative function for a seven data point window. The second-derivative of a spectrum narrows the broad amide I band into its various components, which are related to the different protein chain conformations (Kumosinski and Unruh, 1996; Bandeekar, 1992; Dong, 1990; Byler and Susi, 1988). Another subtraction was performed when required on the second-derivative spectrum of the sample using a second-derivative water vapor spectrum as reference to remove obvious contributions from the water vapor bands. The spectra were then curve-fitted to determine changes in band areas of the amide I components. The full width att half-maximum (fwhm) of the protein component bands associated with aqueous NaCAS was determined initially and then used for curve-fitting the spectra of the protein/plasticizer systems. The criterion of fixing the fwhm of the component bands to constant values between spectra was based on the assumption that the conformation species in the NaCAS/plasticizer systems are similar to that in the pure protein solution. The distribution of the conformations was calculated as a percentage of the integrated area of the component bands relative to that of the amide I contour between 1710 and 1610 cm^{-1}.

Photoacoustic FTIR (PA-FTIR) was employed in the analysis of the film samples. This is a nondestructive analytical technique with sampling depth generally ~10−15 μm below the sample surface, depending on spectrometer operating conditions and the thermal diffusivity of the sample (Rosencwaig, 1975). Spectra were recorded with a MTEC photoacoustic detector Model 200 attachment. Prior to spectral collection, the samples were dried for 48 h in a desiccator. The films were purged in dry helium for 10−30 min while in the photoacoustic cell compartment to remove any residual water vapor. In addition, a stream of dry N_2 was kept flowing in the spectrometer sample compartment throughout spectral acquisition to ensure a constant dry atmosphere and to remove CO_2. Each spectrum comprises 500 co-added scans collected at 4 cm^{-1} resolution using interferometer velocity of 2.5 kHz. The raw spectra were analyzed in a similar manner as for the solution systems discussed above.

RESULTS AND DISCUSSION

Solution Systems. Although the viscosity of casein and caseinate solutions has been studied previously (Konstance and Strange, 1991; Soloshenko et al., 1984), there appears to be a paucity of data for caseinate/plasticizer systems. The effects of glycerol and PEG on the viscosity of aqueous NaCAS was investigated in this study over a wide concentration range. Figure 1 shows that both plasticizers decrease the viscosity of the caseinate solution. This is explained as an effect of the disruption of the protein−protein and protein−solvent interactions through hydrogen bonding of the plasticizer molecules with the NaCAS chain and water molecules. The reduction in viscosity is attributed to the formation of smaller protein aggregates in the NaCAS/glycerol and NaCAS/PEG systems compared to a solution containing only NaCAS.

Within the NaCAS/glycerol system, the viscosity of the solution increases with glycerol content (Figure 2). The viscosity data in Figure 2 can be described as having regions of near-linear concentration dependence interrupted by discontinuous regions around the turning points marked B, E, and G. The regions associated with viscosity increase, that is, AB, CD, EF, and beyond G, are attributed to changes in the particle size of the protein/plasticizer complexes as glycerol molecules interact with the NaCAS chain. The regions near the turning points are probably connected with variations in the three-dimensional structure of the system as the NaCAS/glycerol particles form larger aggregates. This process is expected to be accompanied by a sharp decrease in the volume of the free solvent and observed as an increase in the system viscosity (Soloshenko et al., 1984) (see regions DE and FG of the viscosity graph in Figure 2).

The viscosity of the NaCAS/PEG system shows a trend similar to that of the NaCAS/glycerol system, with displacement of the turning points. The lower viscosity of the PEG solutions can be partly explained by the smaller particle size of the NaCAS/PEG complex. This is not unexpected as there will always be fewer PEG than glycerol molecules in solutions having similar numbers of plasticizer−oxygen atoms available for coordination. However, the particle size of the NaCAS/PEG and NaCAS/glycerol aggregates will differ because of the difference in plasticizer chain length and ability to interact with the protein. The longer PEG molecule probably promotes protein interchain cross-linking, thus facilitating intermolecular bonding between the protein chains.

The effect of the plasticizers on the viscosity of aqueous NaCAS is also a reflection of the changes that occur in the hydrogen bonding network of the solvent. There is evidence that the water sheath immediately surrounding biological polymers, such as proteins, is structured into regions of strong and weak hydrogen bonding as a response to the patchy hydrophilic and hydrophobic regions on the protein surface (Gekko and Timasheff, 1981; Wiggins, 1995a,b). The properties of water in these regions, including its viscosity, density, and solvation properties, differ (Wiggins, 1995a,b). Glycerol is known to interact strongly with water and is easily incorporated into its hydrogen bonding network (Gekko and Timasheff, 1981), thereby perturbing the

water network surrounding the protein. To regain thermodynamic equilibrium, either a substantial protein conformational change takes place to ensure that all hydrophobic areas are out of contact with the solvent or a redistribution of water and glycerol molecules occurs along the protein surface. The latter is generally expected as the change required of the protein structure is hindered by packing constraints and the fact that the hydrophobic groups are part of the protein skeleton. Previous work (Gekko and Timasheff, 1981) suggests that glycerol molecules can penetrate the hydration sheath to interact with the protein skeleton. However, the interactions are thought to be nonspecific bonding because the strongest effects are observed at high glycerol concentrations (1−4 mol L^{-1}). In addition to the difference in molecular size, PEG will be different from glycerol in terms of its ability to alter the water hydrogen bonding. These concepts help explain the difference in particle size of the NaCAS/glycerol and NaCAS/PEG aggregates.

Changes to the NaCAS conformation are expected with the accommodation of the plasticizer molecules. The sensitivity of the amide I mode ~1645 cm^{-1} to the conformation of the protein is well established (Sire et al., 1997; Kumosinski and Unruh, 1996; Surewicz and Mantsch, 1988; Bandeekar, 1992; Dong et al., 1990; Byler and Susi, 1988; Susi and Byler, 1988) and is used to investigate the caseinate secondary structure. However, much controversy still exists in the literature (Kumosinski and Unruh, 1996) in the assignment of the frequency of the amide I band components to unique secondary structures. In the present study, the amide I band components are assigned to the four main structures, that is, turn, 1670−1700 cm^{-1}; α-helix, 1650−1665 cm^{-1}; random coil, 1641−1649 cm^{-1}; and extended β-sheet, 1620−1640 cm^{-1} (Kumosinski and Unruh, 1996; Bandeekar, 1992; Dong et al., 1990).

The analysis of the amide I band in terms of protein secondary structures is not straightforward (Surewicz et al., 1993). Many methods, such as curve-fitting, Fourier deconvolution, and derivation procedures, have been employed in the literature to quantify protein structural changes (Surewicz and Mantsch, 1988; Byler and Susi, 1988; Dong et al., 1990; Kumosinski et al., 1996). However, each of these techniques has its limitations and should be used with care (Surewicz et al., 1993). Despite this, curve-fitting and second-derivative spectral analysis are still useful for obtaining a qualitative understanding of secondary structural changes in protein systems.

Casein and caseinates are generally classified as unordered proteins, that is, proteins that contain few α-helical and β-structures. In the present study, the random and turn conformations, which can be classified as "unordered structures" (~63%), dominate the protein chain structure in aqueous NaCAS. However, there is some local ordering associated with the α-helix and β-sheet conformations. Similar observations were found in earlier studies on β-casein (Susi and Byler, 1988), although the estimated values of the various conformations differ (see Table 2).

Interaction with glycerol molecules causes little overall perturbation of the conformational distribution associated with aqueous NaCAS (Figure 3). This is expected if the plasticizer−protein interactions are of the nonspecific type (Gekko and Timasheff, 1981). The most distinctive changes in the protein structure relative to aqueous NaCAS occur when the glycerol concentration reaches 250−570 mol of plasticizer−oxygen atoms/mol of NaCAS. In this region, there is a depletion of mainly the random and β-sheet conformations in favor of turn structures (380 and 570 mol of plasticizer−oxygen atoms/mol of NaCAS). This is followed by a region (600−850 mol of plasticizer−oxygen atoms/mol of NaCAS) dominated by the random conformation, which appears to form at the expense of the turn conformations. The relative amounts of β-sheet and turn structures increase between 850 and 1025 mol of plasticizer−oxygen atoms/mol of NaCAS. The regions associated with the largest structural changes (380, 570, and ~900 mol of plasticizer−oxygen atoms/mol of NaCAS) can be correlated to the discontinuous regions in the viscosity data for the glycerol system (Figure 2), illustrating that the variation in protein conformation accompanies viscosity change.

Table 2. Comparison of Conformational Estimates of NaCAS and β-Casein

protein	% α-helix	% β-sheet	% other[a]	ref[e]
β-casein[b]	7	19	74	1
β-casein[c]	7	21	72	1
NaCAS (aq)	16	15[d]	69	2

[a] Random coil and turn conformations. [b] As determined in the solid state by Raman spectroscopy. [c] As determined in the solid state by FTIR spectroscopy. [d] Calculated on the basis that the β-sheet structure gives rise to only the 1632 cm^{-1} component. [e] References: 1, Susi and Byler (1988b); 2, present study.

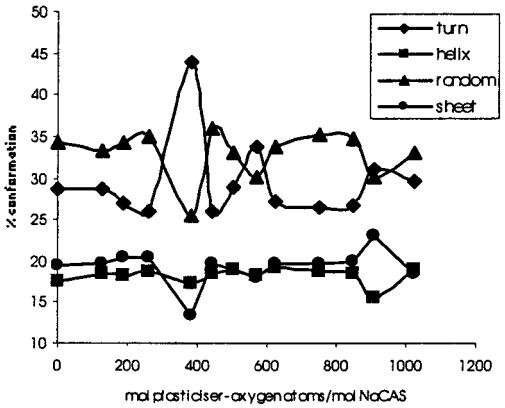

Figure 3. Change in protein conformational structure in NaCAS/glycerol solutions calculated from curve-fit spectral data.

PEG has a lesser effect than glycerol on the protein structure compared to the glycerol system (Figure 4). The smaller variation in protein structure is attributed to weaker NaCAS−plasticizer interactions. The dominant structural changes in the PEG systems are found between 190 and 300 mol of plasticizer−oxygen atoms/mol of NaCAS and 775−850 mol of plasticizer−oxygen atoms/mol of NaCAS. In the first region, the change in conformation structure appears to be between the helix and sheet conformations in favor of the random structure, whereas in the second region, the turn and helix conformations dominate. Again these changes occur in the vicinity of the turning points of the viscosity data.

Film Systems. The tensile strength and elongation-at-break trends for the NaCAS/glycerol and NaCAS/PEG films are shown in Figures 5 and 6. The results are presented in the form of scatterbands to show the natural variation in the data. The borders of the bands are defined by the lowest and highest experimental values obtained. The plasticizer concentration of the

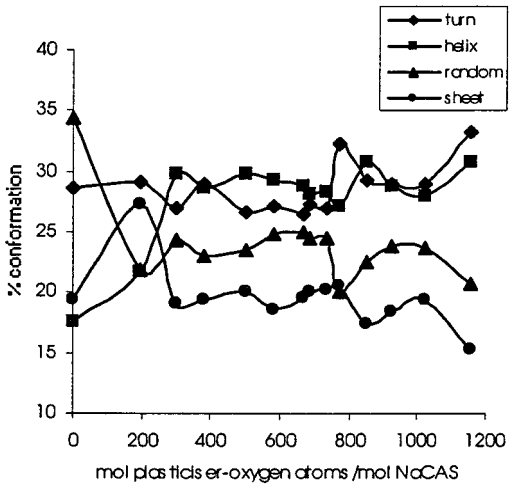

Figure 4. Change in protein conformational structure in NaCAS/PEG solutions calculated from curve-fit spectral data.

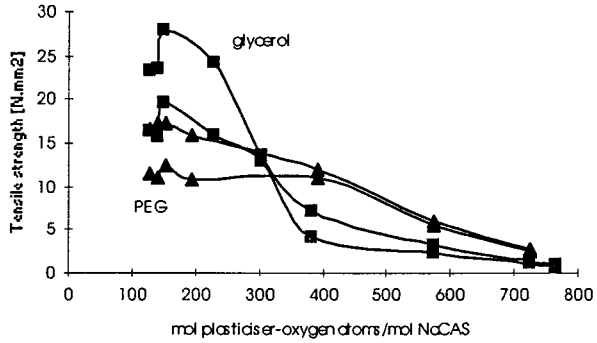

Figure 5. Tensile strength of NaCAS/glycerol and NaCAS/PEG films (23 °C and 50% RH).

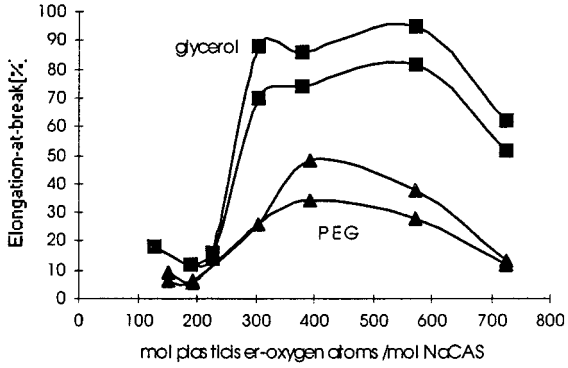

Figure 6. Elongation-at-break of NaCAS films containing glycerol and PEG (23 °C and 50% RH).

films investigated falls between 125 and 770 mol of plasticizer−oxygen atoms/mol of NaCAS. Films outside this range are either too brittle (<129 mol of plasticizer−oxygen atoms/mol of NaCAS) or too tacky (>750 mol of plasticizer−oxygen atoms/mol of NaCAS) to give accurate tensile measurements. An approximate estimate of the tensile strength of the unplasticized NaCAS film is 13.25 ± 5.45 N mm^{-2}.

The tensile strength of the NaCAS films decreases with increasing plasticizer content (Figure 5). Glycerol has a larger effect, the tensile strength changing by ∼20 N mm^{-2} over the plasticizer concentration range studied. The corresponding change caused by PEG is only ∼10 N mm^{-2}. The data can be modeled by eq 3, known as Peleg's model (Peleg, 1994; Roos et al., 1996), to characterize and compare the transition pattern from

Table 3. Dependency of Glass Transitions in NaCAS as a Function of Plasticizer

plasticizer	eq	a_X[a]	X_S[a]
glycerol	$\ln[(Y_S - Y) - 1] = 0.0069X - 2.4099$ $r^2 = 0.9924$	145	306
PEG	$\ln[(Y_S - Y) - 1] = 0.0102X - 5.5742$ $r^2 = 0.9784$	98	546

[a] The units of a_X and X_S are moles of plasticizer−oxygen atoms per mole of NaCAS.

a glassy (high modulus) to a rubbery (low modulus) film in the two systems. This is an alternative to the Williams−Landel−Ferry model that describes the relationship of mechanical changes in biomaterials at and around their glass transition.

$$\ln[(Y_S - Y) - 1] = b + (X/a_X) \quad (3)$$

In eq 3 (Peleg, 1994), the tensile strength (Y) as a function of plasticizer concentration (X) is related to its value at a reference state (Y_S) and a constant (a_X), which is a measure of the broadness of the transition. The reference state is the tensile strength value for an unplasticized or glassy film; it is approximated here as the tensile strength associated with the pure NaCAS film, that is, $Y_S = 13.25$ N mm^{-2}. The reference value, X_S, obtained from $b = -X_S/a_X$, indicates the value for the plasticizer concentration that decreases the tensile strength to 50% below Y_S (Peleg, 1994).

The curve-fit parameters for eq 3, for glycerol- and PEG-plasticized systems, are given in Table 3. The characteristics of the theoretically estimated glass−rubber transition are clearly different for the two systems. The glass transition in the glycerol films is 240 mol of plasticizer−oxygen atoms/mol of NaCAS lower in concentration than for the PEG system. The model also indicates that the transition in the glycerol films occurs over a broader plasticizer range, suggesting that the PEG system is more structured in terms of a more homogeneous bonding distribution.

The percent elongation-at-break of the films increases with plasticizer concentration (Figure 6). Again, glycerol shows a more pronounced effect than PEG. There is an abrupt increase in elongation of ∼65% between 200 and 400 mol of plasticizer−oxygen atoms/mol of NaCAS in the glycerol system, which is halved in the PEG films. The elongation decreases as the plasticizer content in the films is >575 mol of plasticizer−oxygen atoms/mol of NaCAS, regardless of plasticizer.

A possible explanation for the differences in tensile strength and elongation is based on the chain length of the plasticizer and the distribution of hydrogen bonding sites along the NaCAS chain. The hydrophobicity of the amino acid side chains along the protein skeleton determines the various intra- and interchain bonding interactions that can occur in protein molecules and between the protein chain and other entities (Fennema, 1985). In this study, the hydrophobicity distribution of the amino acid side chains along the NaCAS backbone was determined using the hydrophobicity values of amino acids given by Fennema (1985) and based on the molecular sequence (Brunner, 1977) of the three major casein components (α, β, and κ) using a weighted average of the α:β:κ ratio of 10:7:3 for casein (Kinsella, 1984). This approximation assumes that there is minimal difference between the peptide sequence of casein and its ester form. The average hydrophobicity of NaCAS, $G°(\text{NaCAS})_{av}$, was found to be 5.492 kJ mol^{-1}

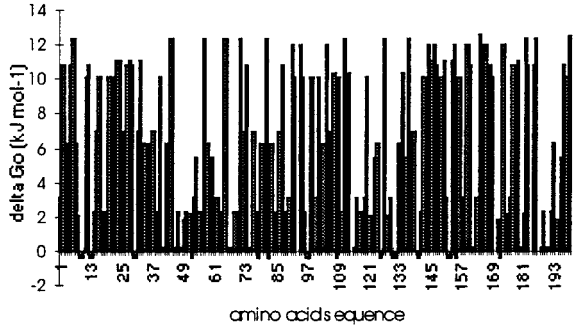

Figure 7. Side-chain hydrophobicity distribution of α-caseinate.

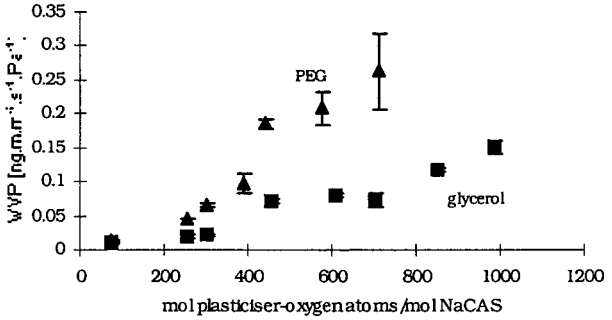

Figure 8. Water vapor permeability (WVP) of NaCAS/glycerol and NaCAS/PEG films (20 °C and 45% RH).

[where $G°(\text{NaCAS})_{av} = [1/n]\Sigma_1^n \Delta G°$ (amino acid side chains) and the value for $\Delta G°$ (amino acid side chains) is obtained from Fennema (1985)]. This value is within the range reported previously for α_{s1}-casein ($G° = 5$ kJ mol^{-1}) and casein ($G° = 6.71$ kJ mol^{-1}) (Fennema, 1985).

The hydrophobic amino acid side chains were found to be more or less evenly distributed throughout the skeleton of the α-caseinate chain (Figure 7). Similar patterns were found for the β- and κ-caseinate components. In each case, there are regions of alternating high- and low-hydrophobicity residues, which will affect the bonding capability of the caseinate chain. The hydrophobicity of the amino acid segments on the protein chain can be compared to the value associated with valine [$\Delta G°(\text{Val}) = 7.050$ kJ mol^{-1}] to determine the possible hydrophilic bonding sites, assuming that valine is the simplest amino acid without effective hydrogen bonding sites for interaction with either glycerol or PEG. Hence, amino acid residues with $\Delta G° < 7.050$ kJ mol^{-1} are assumed to be hydrophilic as these possess groups (NH, C═O, OH, and SH) conducive for hydrogen bonding to the hydroxy and ether oxygen sites. Side chains that are regarded as hydrophobic segments are associated with $\Delta G° > 7.050$ kJ mol^{-1}; these are the long or branched alkyl chains and aromatic groups. The hydrogen bonding groups on these amino acid segments are generally shielded from interacting with other molecules (Fennema, 1985).

It appears that there are more bonding sites along the caseinate skeleton accessible to glycerol than PEG. Glycerol can be easily inserted between the side chains because of its smaller size (Gontard et al., 1993) and, therefore, glycerol has a higher probability of hydrogen bonding at all hydrophilic locations, that is, the low-hydrophobicity sites. Direct interactions of the protein chains in the NaCAS/glycerol films are thus reduced and intermolecular spacing is increased (Gontard et al., 1993), facilitating movement of the protein chains under stress. Conversely, the larger size of PEG may prevent it from interacting with some of the hydrophilic sites on the protein chain due to steric hindrance from neighboring side chains (e.g., the side chains in locations between 1 and 10 in Figure 7). Hence, PEG should be less effective in disrupting the protein-to-protein interactions in films. In addition, PEG is more likely to cross-link protein chains and promote interchain hydrophobic bonding (as discussed previously for the solution system). At high plasticizer concentrations, both the glycerol and PEG films lose ductility and the tensile strength decreases. This is attributed to a loss of cohesiveness in the film network as the number of plasticizer−plasticizer bonds increases.

The WVP of both the glycerol and PEG systems increases with plasticizer concentration (see Figure 8), and the films containing PEG have higher WVP at all similar plasticizer−oxygen concentrations. This can be explained in terms of differences in film molecular packing. Estimates of conformational structure in the film systems obtained by curve-fitting methods indicated that the protein chain in the unplasticized NaCAS film mainly adopts turn structures with a substantial amount of helical and sheet content. As the turn and random conformations were the dominant features in the NaCAS solution phase, it appears that the protein chains become more ordered in the film phase. This is not surprising as the increase in chain ordering probably optimizes the molecular packing in the condensed phase.

Addition of PEG and glycerol changed the distribution of the various NaCAS chain conformations, with glycerol causing larger perturbations from the conformational pattern associated with the protein-only film. There was little change in the proportion of the coil and β-sheet structures between the two plasticizer systems. The main structural variations were associated with the distribution of the helix and random conformational structures and are found at ∼400−700 mol of plasticizer−oxygen atoms/mol of NaCAS. This is near the inflection regions in the WVP data (300−500 mol of plasticizer−oxygen atoms/mol of NaCAS).

At similar plasticizer−oxygen content in these regions (400−700 mol of plasticizer−oxygen atoms/mol of NacAS), the percentage of α-helical structures is higher in the NaCAS/glycerol films than in the NaCAS/PEG films. The formation of the helical structures appears to be at the expense of the random coil conformation. The WVP data [WVP(PEG) > WVP(glycerol)] and protein conformational change (% helix, glycerol > PEG; % random coil, glycerol < PEG) suggest that the random coil structure forms a more "open" molecular network that facilitates water transport.

The higher WVP of the PEG films compared to the glycerol system can also be partly associated with the hydration of the plasticizers. At similar plasticizer content, the number of water molecules that can associate with PEG is higher than with glycerol. If only the two hydrogen bond-active end groups in each plasticizer molecule are unavailable for coordination with water molecules, there will be ∼16 more water molecules associated with PEG than with glycerol. This is because there are eight ether oxygen sites along the PEG chain and each of these can coordinate with at least two water molecules (Phillies and Ren, 1993). In the case of glycerol, there is only one OH group left for interacting with the water molecules. Hence, it is likely that the PEG system is more effective in attracting

water molecules to the film surface and, hence, initiating water transmission.

Inflection regions are found in the WVP data of the NaCAS/plasticizer systems between 300 and 500 mol of plasticizer−oxygen atoms/mol of NaCAS. This is in the vicinity of the glass−rubber transition calculated earlier. The onset of the transition was estimated at 306 mol of plasticizer−oxygen atoms/mol of NaCAS in the glycerol system, on the basis of the tensile strength data, and the midpoint of the WVP inflection region is estimated at 378 mol of plasticizer−oxygen atoms/mol of NaCAS. In the case of the PEG system, these values are 546 and 421 mol of plasticizer−oxygen atoms/mol of NaCAS, respectively. The results clearly show the effect of the glass transition on the WVP properties of the films. It is also interesting to note that the inflection regions in the WVP and the turning points in the viscosity curves coincide, particularly for the NaCAS/glycerol system (Figures 2 and 8). This suggests a possible relationship between the solution and the film phases that may be helpful for screening formulations which will result in particular physical properties.

Comparison with Other Edible and Synthetic Film Systems. The plasticizer size and the effectiveness of the interaction between plasticizer and protein are important factors in determining the physical properties of plasticized NaCAS films. Similar ideas have been invoked in the literature to explain the differences in film strength and permeability of other plasticized biopolymer systems, including γ-irradiated caseinate (propylene glycol and triethylene glycol) (Mezgheni, 1998), whey/protein (glycerol vs sorbitol) (McHugh and Krochta, 1994b), and grain/protein (glycerol vs PEG) (Park, H. J., et al., 1994) films. The ability of the plasticizer to change the physical and water permeability properties of the film depends largely on the compatibility between the plasticizing material and the protein. The actual effect of two plasticizers on a protein is difficult to deduce in most of the published literature because comparisons are usually carried out on a weight protein/weight plasticizer basis, which does not necessarily take into account the properties and number of active sites on each plasticizer molecule. In addition, some properties (such as elongation) are affected by variations in film thickness.

Tables 4 and 5 list some tensile and WVP values for a selection of milk-based edible and synthetic films. The tensile and WVP properties of the NaCAS/glycerol and NaCAS/PEG films are comparable to the values obtained for the other biopolymer films. Depending upon the formulation, the tensile strength of the NaCAS films in the present study can be as high as for polyethylene (high- and low-density phases), illustrating the suitability of glycerol and PEG as plasticizers for NaCAS films.

Edible films, in general, are poor water barriers compared to synthetic films, and NaCAS/glycerol and PEG films are typical in that respect. The WVP values in Table 5 show that a plasticizer can enhance or retard moisture permeation, depending upon its concentration (Banker et al., 1966). The good moisture barrier properties that are needed in edible films designed for fresh produce cannot be achieved using plasticizers alone. However, a combination of protein cross-linking (Avena-Bustillos and Krochta, 1993; Mezgheni et al., 1998) and the incorporation of lipids (McHugh and Krochta, 1994a; Avena-Bustillos and Krochta, 1993) as well as plasticizers could perhaps be the route for attaining this goal.

Table 4. Comparison of Tensile Strength and Elongation-at-Break of Various Edible and Synthetic Packaging Films

film[a]	test conditions (temp, °C; RH, %)	TS[b] (N mm^{-2})	E[b] (%)	ref[c]
α_{s1}-casein/glycerol (49:1)[d]		4.1	38	1, 2
α_{s1}-casein/glycerol (49:1), transglutaminase treated		10.6	77	1, 2
WPI/glycerol (5.7:1)	23; 50	29.1	4.1	1, 3
WPI/glycerol (2.3:1)	23; 50	13.9	30.8	1, 3
WPI/sorbitol (2.3:1)	23; 50	14.0	1.6	1, 3
WPI/sorbitol (1:1)	23; 50	14.7	8.7	1, 3
WG/PEG (2.48:1)	25; 50	5.7	7	4
WG/glycerol (2.2:1)	25; 50	4.4	142	4
NaCAS/glycerol (4:1) [190][e]	23; 50	17.4−26.7	10.5	5
NaCAS/glycerol (2:1) [380]	23; 50	10.9−11.7	73.7−84.2	5
NaCAS/PEG (4.54:1) [129]	23; 50	10.9−16.35	5.3	5
NaCAS/PEG (1.9:1) [304]	23; 50	10.9−13.9	25.4	5
LDPE	23; 50	13	500	1
HDPE	23; 50	26	300	1

[a] WPI, whey protein isolate; WG, wheat gluten; LDPE, low-density polyethylene; HDPE, high-density polyethylene. [b] TS = tensile strength; E = elongation-at-break. [c] References: 1, McHugh and Krochta (1994a); 2, Motoki et al. (1987); 3, McHugh and Krochta (1994b); 4, Park, H. J., et al. (1994); 5, present study. [d] Ratio in parentheses refers to the weight ratio of protein to plasticizer. [e] Ratio in brackets refers to plasticizer concentration in moles of plasticizer−oxygen atoms per mole of NaCAS.

Table 5. Water Vapor Permeability of Various Biopolymeric and Synthetic Films

film[a]	test conditions[b] (temp, °C; RH, %)	P[c]	d[d]	ref[e]
NaCAS	25; 0/81	0.42	0.083	1
NaCAS (buffer treated, pH 4.6)	25; 0/86	0.26	0.072	1
CaCAS	25; 0/85	0.32	0.082	1
CaCAS (buffer treated, pH 4.6)	25; 0/83	0.24	0.072	1
NaCAS/AMG (0.25:1)[f]	25; 0/84	0.18	0.040	1
NaCAS/AMG (4:1)	25; 0/88	0.29	0.094	1
NaCAS/lauric acid (4:1)	25; 0/92	0.11	0.074	2
WPI/glycerol (1.6:1)	25; 0/11	0.076	0.11	2, 3
WPI/glycerol (1.6:1)	25; 0/65	1.39	0.12	2, 3
WPI/glycerol (4:1)	25; 0/77	0.81	0.13	2, 3
NaCAS/glycerol (0.89:1)[f] [850][g]	20; 45/0	0.1313	0.104 ± 0.012	4
NaCAS/glycerol (1.67:1) [455]	20; 45/0	0.0625	0.072 ± 0.013	4
NaCAS/glycerol/palmitic acid (1:0.58:0.25) [440]	20; 45/0	0.0212	0.081 ± 0.021	4
NaCAS/PEG (0.81:1) [710]	20; 45/0	0.26	0.099 ± 0.018	4
NaCAS/PEG (1.32:1) [440]	20; 45/0	0.17	0.071 ± 0.011	4
cellophane	38; 90/0	0.084		2
poly(vinyl chloride)	100−90/0	7.1e^{-4}		5
LDPE	100−90/0	5.5e^{-4}		5
HDPE	38; 90/0	2.31e^{-4}		2

[a] AMG, acetylated monoglyceride; WPI, whey protein isolate; PW, present work; HDPE, high-density polyethylene. [b] Relative humidities (RH) were those on the outside and inside of the test cup, respectively, that is,, outside/inside. [c] Permeability in ng·m/m^2·Pa·s. [d] Film thickness in mm. [e] References: 1, Avena-Bustillos and Krochta (1993); 2, McHugh and Krochta (1994a); 3, Phillies and Ren (1993); 4, present work; 5, Park and Chinnan (1995). [f] Ratio in parentheses refers to the weight ratio of protein to plasticizer. [g] Ratio in brackets represents the plasticizer concentration in moles of plasticizer−oxygen atoms per mole of NaCAS.

Conclusions and Future Work. Glycerol and PEG plasticized NaCAS films have good tensile properties that, if coupled with better water barrier properties, will form effective coatings for use with fresh produce. The results illustrate the effect of the two plasticizers on the properties of NaCAS in the solution and film phases. The interaction of glycerol and PEG with NaCAS is influenced by the size of the plasticizer and the bonding compatibility between the protein and the plasticizer molecule. These concepts have been used to explain the variations in viscosity and tensile properties of the glycerol/NaCAS and PEG/NaCAS systems.

The parameters that characterize the glass−rubber transition of the films indicate that the transition in the PEG system occurs over a smaller plasticizer concentration range. This is taken as an indication of a more homogeneous bonding network in the PEG system compared to the glycerol films, and that conclusion is supported by infrared analysis. Infrared spectral results showed that there is less variation in the structure of the protein chain in the PEG films compared to the glycerol systems. The molecular structure can also be related to changes in the WVP of the films. A larger degree of random coil segments was found in the films in the inflection region of the WVP curve, where a sudden increase in water transmission occurs, indicating that this structure forms an open packing network conducive for water transport.

Interestingly, there appears to be a relationship between the discontinuous regions in the viscosity of the solutions and the tensile and WVP data of the films. The thrust for future work is to investigate this relationship to determine if solution properties can be used as a screening technique to identify regions of unique physical properties in the film phase when new formulations are developed. The molecular structural work performed here has shown some interesting results that can be extended for other edible film systems (Siew et al., 1998).

ABBREVIATIONS USED

FTIR, Fourier transform infrared; FWHM, full width at half-maximum; MW, molecular weight; NaCAS, sodium caseinate; PEG, poly(ethylene glycol) (MW = 400); RH, relative humidity; WVP, water vapor permeability.

ACKNOWLEDGMENT

We thank the New Zealand Dairy Board for their donation of sodium caseinate and John Seakins and Anthony Hayes for technical discussions as well as assistance.

LITERATURE CITED

ASTM D882-91. Standard test methods for tensile properties of thin plastic sheeting. In *Annual Book of American Standard Testing Methods*; ASTM: Philadelphia, PA, 1991; pp 313−321.

ASTM E96-80. Standard test methods for water vapor transmission of materials. In *Selected ASTM Standards on Packaging*; ASTM: Philadelphia, PA, 1984.

Avena-Bustillos, R. J.; Krochta, J. M. Water vapor permeability of caseinate-based edible films as affected by pH, calcium cross-linking and lipid content. *J. Food Sci*. **1993**, 58 (4), 904−907.

Avena-Bustillos, R. J.; Cisneros-Zevallos, L. A.; Krochta, J. M.; Saltveit, M. E. Optimization of edible coatings on minimally processed carrots using response surface methodology. *Trans. ASAE* **1993**, 6 (3), 801−805.

Avena-Bustillos, R. J.; Krochta, J. M.; Saltveit, M. E.; Rojas-Villegas, R. J.; Sauceda-Perez, J. A. Optimization of edible coating formulations on zucchini to reduce water loss. *J. Food Eng*. **1994**, *21*, 197−214.

Bandeekar, J. Amide modes and protein conformation. *Biochim. Biophys Acta* **1992**, *1120*, 123−143.

Banker, G. S.; Gore, A. Y.; Swarbrick, J. Water vapor transmission properties of free polymer films. *J. Pharm. Pharmacol*. **1966**, *18*, 457−466.

Brunner, J. R. Milk Proteins. In *Food Proteins*; Whitaker, J. R., Tannenbaum, S. R., Eds.; AVI Publishing: Westport, CT, 1977; Chapter 7, pp 175−189.

Byler, D. M.; Susi, H. Application of computerized infrared and Raman spectroscopy to conformation studies of casein and other food proteins. *J. Ind. Microbiol*. **1988**, *3*, 73−88.

Debeaufort, F.; Quezada-Gallo, J.-A.; Voilley, A. Edible films and coatings: Tomorrow's packagings: A review. *Crit. Rev. Food Sci*. **1998**, *38* (4), 299−313.

Dong, A.; Huang, P.; Caughey, W. S. Protein secondary structures in water from second-derivative Amide I infrared spectra. *Biochemistry* **1990**, *29*, 3303−3308.

Fennema, O. R. *Food Chemistry*; Dekker: New York, 1985; pp 253−266.

Gekko, K.; Timasheff, S. N. Mechanism of protein stabilization by glycerol: Preferential hydration in glycerol-water mixtures. *Biochemistry* **1981**, *20*, 4667−4676.

Gennadios, A.; McHugh, T. H.; Weller, C. L.; Krochta, J. M. Edible coatings and films based on proteins. In *Edible Coatings and Films to Improve Food Quality*; Krochta, J. M., Baldwin, E. A., Nisperos-Carriedo, M. O., Eds.; Technomic: Basel, Switzerland, 1994.

Gontard, N.; Guilbert, S.; Cuq, J.-L. Water and glycerol as plasticisers affect mechanical and water barrier properties of an edible wheat gluten film. *J. Food Sci*. **1993**, *58* (1), 206.

Kinsella, J. E. Milk proteins: Physicochemical and functional properties. *CRC Crit. Rev. Food Sci. Nutr*. **1984**, *21* (3), 197−262.

Konstance, R. P.; Strange, E. D. Solubility and viscous properties of casein and caseinates. *J. Food Sci*. **1991**, *56* (2), 556−559.

Krochta, J. M.; Pavlath, A. E.; Goodman, N. Edible films from casein-lipid emulsions for lightly-processed fruits and vegetables. In *Engineering and Food*; Elsevier Science: New York, 1990; Vol. 2, pp 329−340.

Krochta, J. M.; Baldwin, E. A.; Nisperos-Carriedo, M. O. *Edible Coatings and Films to Improve Food Quality*; Technomic: Basel, Switzerland, 1994.

Kumosinski, T. F.; Unruh, J. J. Quantitation of the global secondary structure of globular proteins by FTIR spectroscopy: comparison with X-ray crystallographic structure. *Talanta* **1996**, *43*, 199−219.

Madden. *Anal. Chem*. **1978**, *50*, 1383−1386.

McHugh, T. H.; Krochta, J. M. Milk-protein-based edible films and coatings. *Food Technol*. **1994a**, Jan, 97−103.

McHugh, T. H.; Krochta, J. M. Sorbitol- vs glycerol-plasticized whey protein edible films: Integrated oxygen permeability and tensile property evaluation. *J. Agric. Food Sci*. **1994b**, *42*, 841−845.

Mezgheni, E.; D'Aprano, G.; Lacroix, M. Formation of sterilized edible films based on caseinates: Effects of calcium and plasticisers. *J. Agric. Food Chem*. **1998**, *46*, 318−324.

Miller, K. S.; Krochta, J. M. Oxygen and aroma barrier properties of edible films: A review. *Trends Food Sci. Technol*. **1997**, *8* (7) 228−238.

Motoki, M.; Aso, H.; Seguro, K.; Nio, N. α_{S1}-casein film preparation using transglutaminase. *Agric. Biol. Chem*. **1987**, *51*, 997−1002.

Nisperos, M. O.; Baldwin, E. A. Edible coatings for whole and minimally processed fruits and vegetables. *Food Aust*. **1996**, *48* (1), 27−31.

Nussinovitch, A.; Lurie, S. Edible coatings for fruits and vegetables. *Postharvest News Inf*. **1995**, *6* (4), 53N−57N.

Park, H. J.; Chinnan, M. S. Gas and water vapour barrier properties of edible films from protein and cellulosic materials. *J. Food Eng.* **1995**, *25*, 497−507.

Park, H. J.; Bunn, J. M.; Weller, C. L.; Vergano, P. J.; Testin, R. F. Water vapor permeability and mechanical properties of grain protein-based films as affected by mixtures of polyethylene glycol and glycerin plasticisers, *Trans. ASAE* **1994**, *37* (4), 1281−1285.

Park, J. W.; Testin, R. F.; Park, H. J.; Vergano, P. J.; Weller, C. L. Fatty acid concentration effect on tensile strength, elongation and water vapour permeability of laminated edible films. *J. Food Sci.* **1994**, *59* (4), 916−919.

Peleg, M. A model of mechanical changes in biomaterials at and around their glass transition. *Biotechnol. Prog.* **1994**, *10*, 385−388.

Phillies, G. D. J.; Ren, S. Z. Probe diffusion in the presence of nonionic amphiphiles: Triton-X 100. *J. Phys. Chem.* **1993**, *97*, 11563−11568.

Roos, Y. H.; Karel, M.; Kokini, J. L. Glass transitions in low moisture and frozen foods. *Food Technol.*, **1996**, Nov, 95−108.

Rosencwaig, A. Photoacoustic spectroscopy: A new tool for investigation of solids. *Anal. Chem.* **1975**, *47* (6), 592−875.

Savitsky, A.; Golay, M. J. E. Smoothing and differentiation of data by simplified least squares procedures. *Anal. Chem.* **1964**, *36*, 1627−1639.

Siew, D. C. W.; Hayes, A. J.; Donnely, S.; Easteal, A. J.; Cooney, R. P. *Zein-Based Edible Coating Systems: Solution and Films*; **1999**, publication in preparation.

Sire, O.; Zentz, C.; Pin, S.; Chinsky, L.; Turpin, P.-Y.; Martel, P.; Wong, P. T. T.; Alpert, B. Long-range effects in liganded hemoglobin investigated by neutron and UV Raman scattering, FTIR and CD spectroscopies. *J. Am. Chem. Soc.* **1997**, *119*, 12095−12099.

Soloshenko, V. M.; Sergeev, V. A.; Bezrukov, M. G. Structure of protein solutions. Part 1. Investigation and interpretation of viscosity anomalies. *Nahrung* **1984**, *28* (5), 459−472.

Surewicz, W. K.; Mantsch, H. H. New insight into protein secondary structure from resolution-enhanced infrared spectra. *Biochim. Biophys. Acta* **1988**, *952*, 115−130.

Surewicz, W. K.; Mantsch, H. H.; Chapman, D. Determination of protein secondary structure by Fourier transform infrared spectroscopy: A critical assessment. *Biochemistry* **1993**, *32*, 389−394.

Susi, H.; Byler, D. M. Fourier deconvolution of the Amide 1 band of proteins as related to conformation. *Appl. Spectrosc.* **1988**, *42* (5), 819−826.

U.S. FDA. *U.S. FDA Food Additives Status List*; U.S. GPO: Washington, DC, 1997.

Wiggins, P. M. Micro-osmosis in gels, cells and enzymes. *Cell Biochem. Funct.* **1995a**, *13*, 165−172.

Wiggins, P. M. High and low-density water in gels. *Prog. Polym. Sci.* **1995b**, *20*, 1121−1163.

Received for review June 10, 1998. Revised manuscript received June 4, 1999. Accepted June 9, 1999. D.C.W.S. was supported by the New Zealand Science and Technology Post-Doctoral Fellowship Programme.

JF9806311